Journal of Electronics, Electromedical Engineering, and Medical Informatics
Homepage: jeeemi.org; Vol. 8, No. 2, April 2026, pp: 789-805 e-ISSN: 2656-8632

RESEARCH ARTICLE OPEN ACCESS

Processing and Analysis of Electrogastrogram (EGG) Signals to Evaluate Stressor and Motion Sickness Conditions in Virtual Reality Environments

Mhd. Hanafi, Alvin Sahroni, Sri Kusumadewi, Hendra Setiawan, and Firdaus

Department of Electrical Engineering, Faculty of Industrial Technology, Universitas Islam Indonesia, Yogyakarta, Indonesia

Corresponding author: Firdaus (e-mail: firdaus@uii.ac.id), Author(s) Email: Mhd. Hanafi (e-mail: 23925011@alumni.uii.ac.id), Alvin Sahroni (e-mail: alvinsahroni@uii.ac.id), Sri Kusumadewi (e-mail: srikusumadewi@uii.ac.id), Hendra Setiawan (e-mail: hendrasetiawan@uii.ac.id)

Abstract **Virtual Reality (VR) technology has rapidly evolved and is widely utilized in healthcare, education, and entertainment. However, its use often induces motion sickness and stressor, which may reduce user comfort and performance. This study aims to determine whether VR exposure triggers such conditions, evaluate them using electrogastrogram (EGG) signals, and identify the most effective EGG features as physiological indicators. EGG signals from nine healthy male subjects were recorded using two channels under three experimental conditions (pre, stimulation, and post) during both pre-prandial and post-prandial phases. Frequency-domain analysis was performed using the Fast Fourier Transform (FFT) within the 0.03-0.07 Hz range to extract dominant frequency, dominant magnitude, mean frequency, average magnitude, and band power. Subjective evaluation was conducted using a five-point Likert scale. The results indicate that VR exposure induced motion sickness and stressor, with Likert scores ranging from 3 to 5. Three normalized magnitude features of the EGG signal on channel 0 during the pre-prandial stimulation phase exhibited significant positive correlations with motion sickness: dominant magnitude ($r = 0.841$, $p = 0.005$), average magnitude ($r = 0.742$, $p = 0.022$), and band power ($r = 0.788$, $p = 0.012$). These features also showed significant correlations with stressor levels: dominant magnitude ($r = 0.895$, $p = 0.001$), average magnitude ($r = 0.780$, $p = 0.013$), and band power ($r = 0.821$, $p = 0.007$). These findings confirm that VR exposure can induce motion sickness and act as a physiological stressor, with three EGG magnitude features serving as reliable physiological indicators. The lower corpus extending to the antrum and pylorus was identified as the most representative electrode placement area, and the pre-prandial phase was found to be more susceptible to VR-induced disturbances than the post-prandial phase.**

Keywords **Virtual Reality (VR); Motion Sickness; Stressor; EGG; Likert Scale.**

I. Introduction

The advancement of technology in the era of the Industrial Revolution 5.0 has fostered innovations that simplify human life through the integration of physical and digital technologies, one of which is Virtual Reality (VR) [1]. VR enables users to interact with computer-simulated three-dimensional environments [2]. Currently, VR is used not only for entertainment but also across various fields, including healthcare, education, manufacturing, and retail sectors [3]. In gaming and entertainment, VR provides immersive experiences and learning opportunities, as demonstrated in applications such as Box VR, shooting games, and sports games [4], [5], [6]. In education, VR enhances learning methods through interactive digital experiences [7], [8]. Meanwhile, in healthcare, VR is applied for surgical procedure simulations and medical training [9], [10].

However, VR may also induce side effects such as motion sickness and stressors, which can decrease user comfort and task performance [11], [12]. Motion sickness occurs due to sensory conflicts or mismatches between visual and vestibular inputs [13], [14], whereas a stressor refers to a physical or psychological stimulus that triggers a stress response [15]. Studies have reported that cybersickness remains a major challenge in VR applications, as it can cause symptoms such as nausea, dizziness, and visual discomfort, which may

Manuscript received 5 February 2026; Revised 15 March 2026; Accepted 20 April 2026; Available online 26 April 2026
Digital Object Identifier (**DOI**): https://doi.org/10.35882/jeeemi.v8i2.1531

reduce user performance and limit the usability of VR systems [16], [17]. Approximately 22-80% of VR users experience cybersickness symptoms [16], while around 40-70% of users may experience motion sickness during VR interaction [17]. In addition, up to 60% of users may develop symptoms within the first 10 minutes of VR exposure [18].

These findings highlight the importance of evaluating motion sickness and stressors during VR exposure to better understand users' physiological responses and support the development of safer, more comfortable VR environments. These conditions can be evaluated subjectively using tools such as the Likert scale [19], [20], [21] or the Simulator Sickness Questionnaire (SSQ) [12], [22], while objective evaluations can be performed using physiological signals such as heart rate, body temperature, and electrogastrogram (EGG) recordings [22], [23]. Subjective assessments are prone to bias because they rely on individual perception, while physiological measurements allow for more accurate and continuous monitoring. Therefore, combining subjective and objective methods provides a more comprehensive evaluation framework [24]. Several previous studies have shown that motion sickness in VR simulations can be evaluated using EGG signals in conjunction with the Simulator Sickness Questionnaire (SSQ) [12], [22]. Other studies have further emphasized the potential of EGG through single-channel frequency-domain analysis under resting conditions, revealing that EGG signals within the 0.03-0.07 Hz frequency range effectively reflect relevant physiological activity [25].

However, existing studies have mostly focused on general EGG responses or questionnaire-based evaluations, and only limited research has examined the relationship between specific frequency-domain EGG features and VR-induced motion sickness and stressor responses. In addition, the identification of the most informative EGG features that can serve as reliable physiological indicators for these conditions remains limited.

Based on this research gap, the problem formulation of this study is defined as follows: (1) whether VR exposure induces motion sickness and stressor responses in users, (2) whether these responses can be objectively evaluated using EGG signals, and (3) which EGG features are the most effective physiological indicators for detecting these conditions. From a physiological perspective, VR exposure is expected to produce measurable responses in gastric electrical activity because sensory conflicts and psychological stress can activate the autonomic nervous system, which directly influences gastrointestinal motility. Therefore, this study hypothesizes that VR stimulation induces motion sickness and stress responses, as reflected in measurable changes in EGG signals, particularly in magnitude-related features. To address these research questions, this study focuses on the frequency-domain analysis of EGG signals using the Fast Fourier Transform (FFT) to extract five primary features: dominant frequency, dominant magnitude, mean frequency, average magnitude, and band power. The purpose of this study is to evaluate the influence of VR exposure on motion sickness and stressor responses, develop an EGG-based evaluation framework for these conditions, and identify reliable EGG features that can serve as physiological markers.

This paper is organized as follows. Section II describes the research methodology. Section III presents the results and analysis. Section IV discusses the physiological interpretation of the findings. Finally, Section V concludes the study and outlines future research directions.

II. Research Method

A. Subjects

This study involved nine healthy male participants aged between 20 and 23 years. The sample size is consistent with previous physiological signal studies that typically involve approximately 8 to 10 participants in controlled experimental settings, thereby supporting the methodological validity of this study [26], [27], [28]. All participants were male in order to maintain physiological homogeneity and to minimize variability caused by biological differences between males and females, particularly in gastrointestinal and autonomic responses that may influence electrogastrogram (EGG) measurements. The age range was limited to young adults (20-23 years) to reduce age-related variability in gastric motility and autonomic nervous system responses, thereby ensuring more consistent physiological conditions during the experiment.

Table 1. Body Mass Index (BMI) Classification.

No	BMI Criteria	Value Range (kg/m²)
1	Underweight	< 18.5 kg/m²
2	Healthy	18.5-22.9 kg/m²
3	Overweight	23.0-27.4 kg/m²
4	Obese	> 27.5 kg/m²

In addition, participant characteristics were described using the Body Mass Index (BMI) classification based on the guidelines of the Ministry of Health of the Republic of Indonesia, as shown in Table 1 [29]. The BMI classification was included to describe the general physical condition of the participants and to support the interpretation of physiological responses

Manuscript received 5 February 2026; Revised 15 March 2026; Accepted 20 April 2026; Available online 26 April 2026
Digital Object Identifier (**DOI**): https://doi.org/10.35882/jeeemi.v8i2.1531

during the experiment. However, BMI was not treated as a primary experimental variable in this study. Participants were instructed to fast for at least 6 hours, including abstaining from both food and beverages, prior to the recording session to ensure consistent gastric conditions during EGG measurement.

The application of this BMI classification aimed to identify and analyze whether BMI influences the occurrence of motion sickness and stressor responses among participants.

B. Data Acquisition Devices

This study utilized several hardware and software components to support the signal acquisition and data analysis processes, as described below:

1. Hardware

The main hardware used in this study was the OpenBCI Cyton Biosensing Board (8-16 channels) with a sampling rate of 250 Hz for EGG signal acquisition. Ag/AgCl surface electrodes were attached to the abdominal skin using medical adhesive to ensure stable contact and to minimize motion artifacts during the recording process. The recorded signals were transmitted and stored on a laptop for further processing and analysis. The Oculus Rift S headset was used as the primary Virtual Reality (VR) device to deliver the experimental stimulation.

2. Software

The OpenBCI GUI application (v6.0.0-beta.1) was used for signal acquisition and data storage. The recorded data were subsequently processed in Python for signal preprocessing, Fast Fourier Transform (FFT) analysis, and feature extraction. Subjective evaluation was conducted using a five-point Likert scale (1 = no symptoms, 5 = very severe) to assess motion sickness and stressor levels. The Epic Roller Coaster VR simulation was used as the stimulation medium because previous studies have demonstrated its effectiveness in inducing motion sickness and stressor responses in VR environments [30], [31].

C. Virtual Reality Modeling (Visual-Vestibular)

Motion sickness in Virtual Reality (VR) is modeled as a result of a mismatch between visual and vestibular information received by the human sensorimotor system. In VR environments, users receive motion-related stimuli primarily through the visual system, while vestibular feedback corresponding to actual body movement is absent or inconsistent. This sensory mismatch generates perceptual conflict, commonly referred to as visual-vestibular sensory conflict, which has been widely identified as a major cause of VR-induced motion sickness [17], [32]. This conceptual framework provides the basis for quantitatively modeling the relationship between sensory input discrepancies and the resulting physiological responses. Mathematically, the sensory conflict is formulated as shown in Eq. (1) [17], [32]:

$$e_a(t) = a_v(t) - a_b(t), e_w(t) = w_v(t) - w_b(t) \quad (1)$$

where $a_v(t)$ and $w_v(t)$ denote the visually perceived linear acceleration and angular velocity derived from VR stimuli, respectively, while $a_b(t)$ and $w_b(t)$ represent the actual linear acceleration and angular velocity of the body. The magnitude of the visual-vestibular conflict is quantified using the conflict index defined in Eq. (2) [17], [32]:

$$C(t) = \sqrt{\alpha||e_a(t)||^2 + \beta||e_w(t)||^2} \quad (2)$$

where α and β are weighting factors representing the relative contributions of linear acceleration and angular velocity mismatches. The dynamics of motion sickness progression during VR exposure are modeled using a first-order differential equation, as expressed in Eq. (3) [17], [32]:

$$\frac{dS(t)}{dt} = k_c C(t) - k_r S(t) \quad (3)$$

where $dS(t)$ represents the level of motion sickness, k_c is the accumulation constant associated with visual-vestibular conflict, and k_r is the physiological recovery constant. This model indicates that cybersickness increases as the sensory conflict accumulates and decreases over time due to adaptive recovery mechanisms.

In addition to sensory conflict, exposure to Virtual Reality (VR) can activate the autonomic nervous system, contributing to physical discomfort and psychological stress. Various elements within the VR environment, such as motion speed, virtual height, visual-auditory stimulus intensity, and sudden stimulus events, can elevate users' stress levels, which often co-occur with cybersickness. The stress response is influenced by the intensity of VR and is mathematically formulated in Eq. (4) [33], [34]:

$$\frac{dR(t)}{dt} = k_s U(t) - k_{rs} R(t) \quad (4)$$

where $R(t)$ represents the stress level, $U(t)$ denotes the intensity of VR, k_s is the stress accumulation constant, and $k_{rs}$is the stress recovery constant.

D. Electrode Placement

The EGG signals were recorded using a two-channel configuration. Cutaneous electrogastrography measures gastric electrical activity noninvasively from the abdominal surface; therefore, electrode placement is typically determined based on anatomical landmarks that approximate different gastric regions.

The use of two channels enables the recording of electrical activity from separate abdominal areas representing proximal and distal stomach regions,

Manuscript received 5 February 2026; Revised 15 March 2026; Accepted 20 April 2026; Available online 26 April 2026
Digital Object Identifier (**DOI**): https://doi.org/10.35882/jeeemi.v8i2.1531

allowing better observation of spatial variations in gastric slow-wave activity. Channel 0 was positioned over the lower corpus extending to the antrum and pylorus, following the placement approach described in [35], [36]. Channel 1 was positioned over the fundus and upper corpus regions of the stomach, according to the methods outlined in [37], [38]. The electrode placement configuration for both channels is illustrated in Fig. 1.

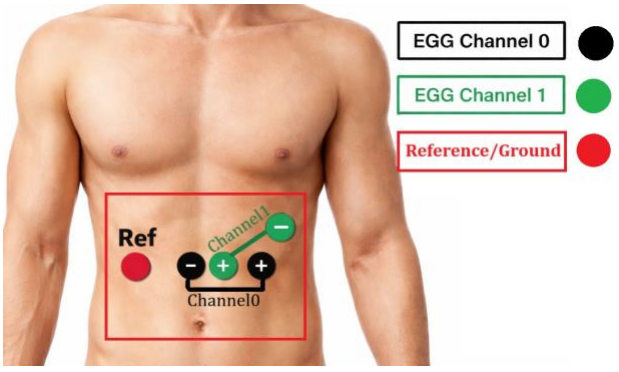

Fig. 1. Electrode Placement

E. Experimental Design and Data Collection

The data collection process was carried out at the Biomedical Laboratory, Department of Electrical Engineering, Universitas Islam Indonesia, using a combination of objective and subjective evaluation methods. In the objective approach, EGG signals were recorded under two physiological conditions: pre-prandial (before eating) and post-prandial (after eating). The experimental design is described as follows. The data collection process began with participants signing an informed consent form, followed by the attachment of a two-channel EGG recording system using OpenBCI. The experiment consisted of two phases, namely the pre-prandial and post-prandial sessions. In the pre-prandial session, the experimental protocol was conducted under fasting conditions. Each session consisted of three consecutive periods: a 10-minute baseline period (pre), a 7-minute VR stimulation period (stim), and an 8-minute post-stimulation recovery period (post), resulting in a total duration of 25 minutes per session. During the baseline (pre) and recovery (post) periods, participants were seated in a comfortable position while observing a blank white screen to obtain resting EGG signals. The stimulation period (stim) consisted of a VR roller coaster simulation designed to induce motion sickness and stress responses.

Upon completion of each period (pre, stim, and post), participants filled out the same Likert scale questionnaire consisting of two questions related to the severity of motion sickness and stressor. The rating scale ranged from 1 (no symptoms) to 5 (very severe symptoms). After completing the pre-prandial session, participants were given 20 minutes to consume a meal, followed by approximately 2 hours of rest in a lying position without engaging in physical activity. The experiment then continued with the post-prandial session, during which the same experimental protocol (pre, stim, and post) was repeated.

F. Preprocessing

The preprocessing stage aimed to remove noise from the EGG signals prior to analysis. This stage included visual inspection of the raw signals and the application of a Finite Impulse Response (FIR) band-pass filter within the 0.03-0.07 Hz frequency range to eliminate baseline drift and high-frequency noise [42], [44]. This frequency range corresponds to the normal gastric slow-wave activity, which typically occurs at 2-4 cycles per minute (cpm) [25], [38]. After filtering, the signals were transformed from the time domain into the frequency domain using the Fast Fourier Transform (FFT) to enable spectral analysis and feature extraction. The FFT efficiently computes the Discrete Fourier Transform (DFT) of a discrete signal and provides a representation of the frequency components contained in the EGG signal [39]. The transformation is defined in Eq. (5) [39] as follows:

$$X[k] = \sum_{n=0}^{N-1} x[n] e^{-j2\pi kn/N} \quad (5)$$

where $x[n]$ represents the discrete EGG signal in the time domain, N is the total number of samples, k denotes the frequency index, and $X[k]$ represents the spectral component of the signal in the frequency domain. Through this transformation, the magnitude spectrum $X[k]$ can be analyzed to extract several frequency-domain features that characterize the physiological responses reflected in the EGG signal [38], [40].

G. Feature Extraction

Feature extraction was performed to obtain numerical parameters in the frequency domain, which were subsequently used for statistical analysis. The extracted features included the following:

1. Dominant Frequency: the frequency component with the highest spectral magnitude within the analysis range of 0.03-0.07 Hz. Eq. (6) shows the calculation of the dominant frequency [38], [40].

$$DF = F_k, where\ k = argmax|X(f)| \quad (6)$$

where Df is the dominant frequency (Hz), F_k is the frequency corresponding to the maximum spectral magnitude, $X(f)$ is the magnitude spectrum obtained from the FFT of the frequency (f), $argmax$ is the index of the maximum magnitude value.

Manuscript received 5 February 2026; Revised 15 March 2026; Accepted 20 April 2026; Available online 26 April 2026
Digital Object Identifier (**DOI**): https://doi.org/10.35882/jeeemi.v8i2.1531

2. Dominant Magnitude: the magnitude at the dominant frequency relative to the total spectral magnitude within the analysis range of 0.03-0.07 Hz. Eq. (7) presents the calculation of the dominant magnitude [38], [39].

$$DM = \max|X(f)| \quad (7)$$

where DM is the highest magnitude in the spectrum (μV), $X(f)$ is the magnitude spectrum obtained from the FFT of the frequency (f), max is the function used to obtain the maximum magnitude value.

3. Mean Frequency: the weighted average value of all frequency components within the analysis range of 0.03-0.07 Hz. Eq. (8) presents the calculation of the mean frequency [38], [39].

$$MF = \frac{\sum_{i=1}^{N} fi \cdot P(fi)}{\sum_{i=1}^{N} P(fi)} \quad (8)$$

where MF is the weighted mean frequency (Hz), fi is the i-th frequency component, $P(fi)$ is the power or magnitude at frequency fi, N is the total number of frequency points in the spectrum.

4. Average Magnitude: the average amplitude of the frequency spectrum within the analysis range of 0.03-0.07 Hz. Eq. (9) presents the calculation of the average magnitude [38], [39].

$$AM = \frac{1}{N}\sum_{i=1}^{N} |X(fi)| \quad (9)$$

where AM is the average magnitude of the spectrum (μV), $X(fi)$ is the magnitude at the i-th frequency point obtained from the FFT, N is the number of frequency points in the spectrum.

5. Band Power: the total power within the 0.03-0.07 Hz frequency band relative to the total spectral power. Eq. (10) presents the calculation of band power [37], [38].

$$BP = \sum_{f_{low}}^{f_{high}} P(f) \cdot \triangle f \quad (10)$$

where BP is the total spectral power within a specific frequency range (μV²), $P(f)$ is the power at frequency f, f_{high} is the lower frequency limit (Hz), f_{low} is the upper frequency limit (Hz), $\triangle f$ is the frequency resolution (Hz).

H. Data Analysis

The subjective responses related to motion sickness symptoms and stressor perception were collected using a five-point Likert scale, where 1 represents the lowest level, and 5 represents the highest level of perceived symptoms. Likert-type scales are widely used in behavioral and experimental research as they provide a structured method for quantifying subjective perceptions such as attitudes, perceptions, and symptom intensity. Previous methodological studies have demonstrated that Likert-type scales offer valid and reliable measurements for capturing subjective responses in quantitative research [41], [42]. In this study, the questionnaire items were developed based on commonly used subjective symptom assessment approaches in VR-related motion sickness research and were reviewed by domain experts to ensure content validity. Pearson correlation analysis was applied to evaluate the linear relationships between physiological EGG features, motion sickness scores, stressor scores, and BMI. Prior to performing Pearson correlation analysis, the normality of the data distribution was evaluated using the Shapiro-Wilk test. The analysis was conducted to evaluate relationships among EGG features, motion sickness scores, stressor scores, and BMI under the pre, stimulation, and post-stimulation conditions during both pre-prandial and post-prandial phases. The tested correlations included Likert scale (motion sickness-stressor), motion sickness-BMI, stressor-BMI, and EGG features-Likert scale (motion sickness/stressor) across both recording channels (0 and 1). This analysis was conducted to examine whether subjective motion sickness responses correspond with physiological changes recorded in the EGG signals. Correlations were considered statistically significant at $p < 0.05$, following the approach used in previous studies [41], [42]. The outcomes of this analysis provide a basis for interpreting the relationship between subjective perception and physiological responses across different experimental conditions.

III. Result

This section presents the results obtained from both subjective evaluations and physiological signal analysis.

A. Subject Demographics

Table 2 summarizes the body mass index (BMI) classification of the participants. Five subjects were classified as having a normal BMI, two subjects were underweight, one subject was overweight, and one subject was categorized as obese. BMI was included as a demographic parameter because it is commonly used as an indicator of nutritional status and general health condition [43]. All participants were confirmed to be in good health and reported no history of gastrointestinal disorders prior to the experiment.

B. Subject Evaluation

Subjective evaluation was conducted using a five-point Likert scale to assess the effects of Virtual Reality (VR) exposure on motion sickness and stressor levels among the participants. The scale ranged from 1 to 5, with higher scores indicating greater symptom

Manuscript received 5 February 2026; Revised 15 March 2026; Accepted 20 April 2026; Available online 26 April 2026
Digital Object Identifier (**DOI**): https://doi.org/10.35882/jeeemi.v8i2.1531

Table 2. Subject Demographics

No	Subject	Height (m)	Weight (kg)	BMI (kg/m2)	Category	Medical History
1	S1	1.81	60	18.31	Underweight	None
2	S2	1.80	70	21.60	Healthy	None
3	S3	1.67	69	24.74	Overweight	None
4	S4	1.68	60	21.26	Healthy	None
5	S5	1.69	60	21.01	Healthy	None
6	S6	1.65	50	18.37	Underweight	None
7	S7	1.69	55	19.26	Healthy	None
8	S8	1.65	85	31.22	Obese	None
9	S9	1.69	62	21.71	Healthy	None

intensity, where scores of 3-5 represent moderate-to-severe conditions. The evaluation results are summarized in Fig. 2 (a)-(d). Data were collected at the end of each experimental phase (pre, stim, and post) to observe variations in perceived discomfort under different conditions. The results show that responses varied across participants, reflecting individual differences in sensitivity to VR exposure. This variation provides additional context for understanding the overall pattern observed in the study.

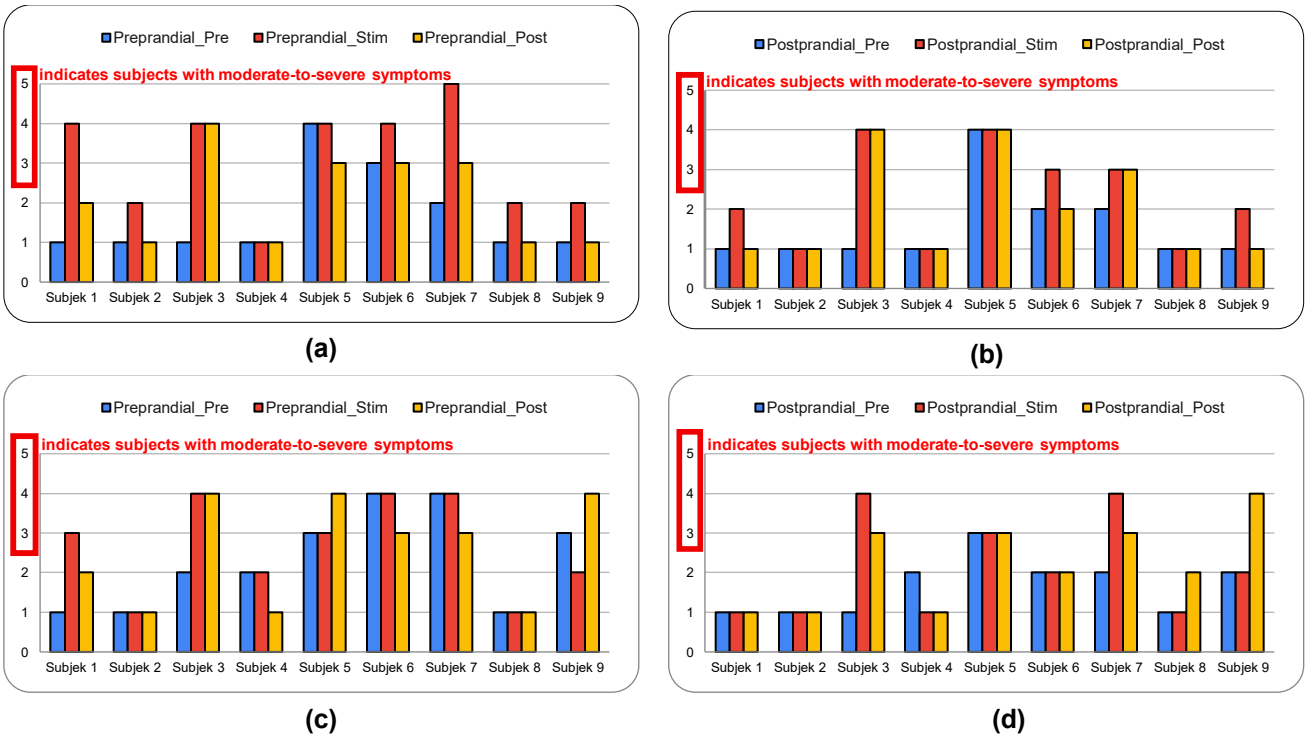

Fig. 2. (a) Motion Sickness in the Pre-prandial Phase, (b) Motion Sickness in the Post-prandial Phase, (c) Stressor in the Pre-prandial Phase, (d) Stressor in the Post-prandial Phase.

In the pre-prandial phase, the motion sickness assessment showed that Subjects 1, 3, 5, 6, and 7 reported moderate to severe symptoms (scores 3-5), accounting for 5/9 subjects (55.6%), while Subjects 2, 4, 8, and 9 reported no or only mild symptoms (scores 1-2), as shown in Fig. 2 (a). In the post-prandial phase, Subjects 3, 5, 6, and 7 again reported moderate to severe symptoms (4/9 subjects; 44.4%), whereas

Manuscript received 5 February 2026; Revised 15 March 2026; Accepted 20 April 2026; Available online 26 April 2026
Digital Object Identifier (**DOI**): https://doi.org/10.35882/jeeemi.v8i2.1531

Subjects 1, 2, 4, 8, and 9 showed no symptoms, as presented in Fig. 2 (b). The assessment of stressor levels showed a similar pattern. In the pre-prandial phase, Subjects 1, 3, 5, 6, 7, and 9 reported moderate to high stressor levels (scores 3-4), corresponding to 6/9 subjects (66.7%), while Subjects 2, 4, and 8 reported very low levels (scores 1-2), as shown in Fig. 2 (c). In the post-prandial phase, Subjects 3, 5, 7, and 9 reported moderate to high stressor levels (4/9 subjects; 44.4%), whereas Subjects 1, 2, 4, 6, and 8 showed low stressor levels, as illustrated in Fig. 2 (d). Further analysis was conducted to examine the relationship between motion sickness and stressor scores using Pearson correlation analysis, and the results are presented in Fig. 3.

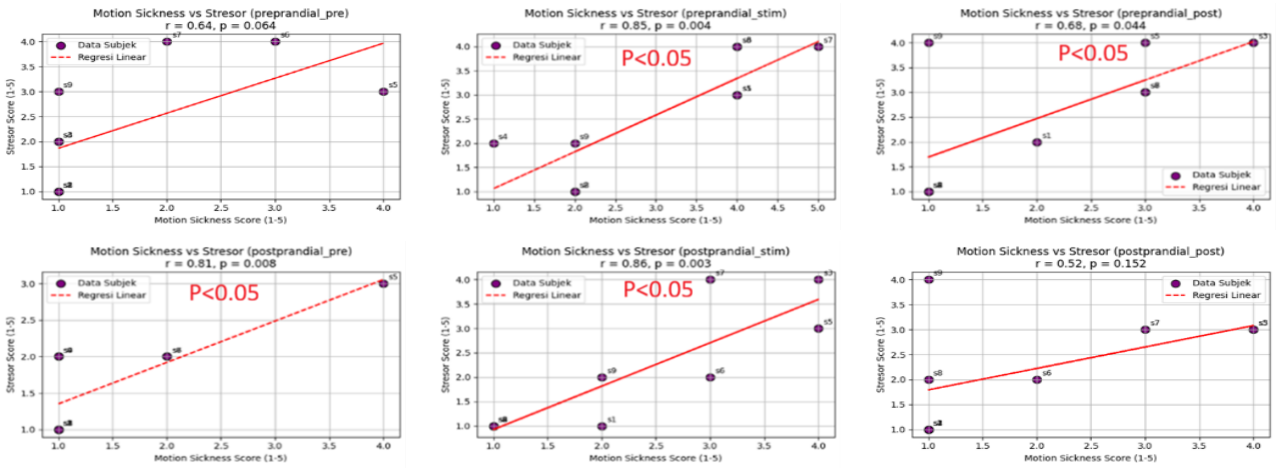

Fig. 3. Correlation Between Motion Sickness and Stressor Scores

Table 3. Correlation Between BMI and Subjective Evaluation Scores

No	Phase	BMI vs Motion Sickness (r,p)	BMI vs Stressor (r,p)
1	Pre-prandial (Pre)	-0.32 (0.398)	-0.48 (0.191)
2	Pre-prandial (Stim)	-0.47 (0.201)	-0.61 (0.080)
3	Pre-prandial (Post)	-0.38 (0.317)	-0.35 (0.361)
4	Post-prandial (Pre)	-0.25 (0.517)	-0.35 (0.362)
5	Post-prandial (Stim)	-0.38 (0.317)	-.0.24 (0.538)
6	Post-prandial (Post)	-0.19 (0.632)	0.05 (0.898)

Pearson correlation coefficients (r) between motion sickness and stressor scores, with $p < 0.05$, indicate statistically significant correlations. In the pre-prandial condition, the strongest correlation was observed during the stimulation phase ($r = 0.85$, $p = 0.004$), followed by the post phase ($r = 0.68$, $p = 0.044$). In the post-prandial condition, similarly strong correlations were found, with the highest during stimulation ($r = 0.86$, $p = 0.003$) and another significant correlation in the pre-phase ($r = 0.81$, $p = 0.008$). These results also indicate statistically significant associations between motion sickness scores and perceived stressor levels ($p < 0.05$). In addition, the relationship between body mass index (BMI) and subjective evaluation scores, including motion sickness and stressor levels, was examined using Pearson correlation analysis. The results of this analysis are summarized in Table 3. The results indicate that all experimental phases yielded p-values greater than 0.05, suggesting that no statistically significant relationships were found between BMI and motion sickness scores, nor between BMI and stressor scores. This finding implies that BMI alone may not be a determining factor influencing susceptibility to motion sickness or perceived stress levels under the given experimental conditions.

C. Signal Processing and Feature Extraction

The next stage involved data processing. The raw EGG signals generally contained various types of noise, originating from power line interference, respiration, cardiac activity, and other external disturbances [44]. Therefore, a Finite Impulse Response (FIR) band-pass filter with a Hamming window and order 201 was applied. This filter was designed to preserve the gastric slow-wave components within the 0.03-0.07 Hz frequency range, following the approach used in previous studies [42], [45]. Following the filtering process, the Fast Fourier Transform (FFT) was employed to analyze the frequency-domain characteristics of the EGG signal, particularly to examine the distribution of spectral power. As illustrated in Fig. 5, the signal processing results for the

Manuscript received 5 February 2026; Revised 15 March 2026; Accepted 20 April 2026; Available online 26 April 2026
Digital Object Identifier (**DOI**): https://doi.org/10.35882/jeeemi.v8i2.1531

postprandial phase are presented in three stages: (a) the raw EGG signal, which still contains significant noise components; (b) the filtered signal after applying the FIR band-pass filter within the 0.03-0.07 Hz range, showing a clearer representation of the gastric rhythm; and (c) the resulting frequency spectrum obtained using FFT, highlighting the dominant frequency components associated with gastric activity.

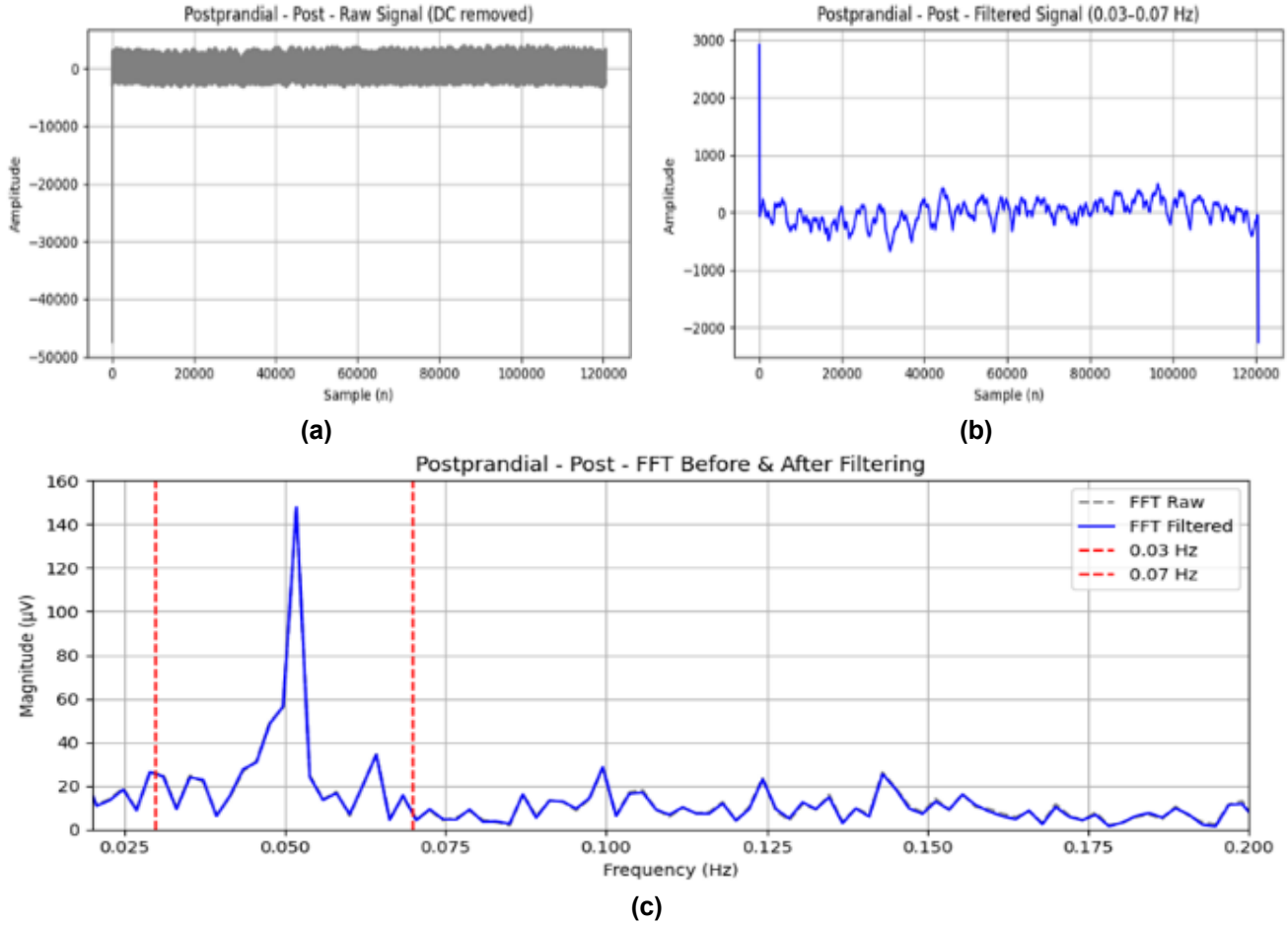

Fig. 4. Illustrates the EGG Signal Processing in the Post-prandial Post Phase for Subject 4 (a) Raw data, (b) Output of FIR band-pass filter (0.03-0.07 Hz), and (c) Frequency spectrum analysis using FFT

Fig. 4 illustrates the EGG signal processing in the post-prandial post phase for Subject 4. This subject was selected due to the high quality of the recorded signal, characterized by low noise levels and a clearly defined slow-wave pattern, with a dominant frequency close to 0.05 Hz. This frequency corresponds to the baseline rhythm of gastric activity, which is known to be the most stable and typically appears clearly under resting conditions, consistent with previous studies [35-37]. The processing stages include: (a) Raw signal, (b) Filtered signal using an FIR band-pass filter within the 0.03-0.07 Hz frequency range, and (c) Frequency spectrum analysis of the filtered signal using FFT.

As shown in Fig. 4(a), the raw EGG signal still contains significant noise components, reflected by irregular fluctuations and high-amplitude variations that obscure the underlying gastric rhythm. After applying the FIR band-pass filter, as presented in Fig. 4(b), the signal becomes noticeably smoother, with non-gastric components effectively attenuated, allowing the slow-wave activity within the target frequency band to be more clearly observed.

In the final stage, as depicted in Fig. 4(c), a prominent magnitude peak is observed within the 0.03-0.07 Hz frequency band, representing gastric slow-wave activity. This indicates that the filtering process successfully preserved the physiologically relevant frequency components while suppressing unwanted noise. Feature extraction was then performed to obtain quantitative parameters representing the frequency-domain characteristics of the EGG signal. The extracted features include dominant frequency, mean frequency, dominant magnitude, average magnitude within the gastric frequency band, and normalized band power.

Manuscript received 5 February 2026; Revised 15 March 2026; Accepted 20 April 2026; Available online 26 April 2026
Digital Object Identifier (**DOI**): https://doi.org/10.35882/jeeemi.v8i2.1531

Table 4 summarizes the descriptive statistics (mean ± standard deviation) of the extracted EGG features across all subjects (1-9) for each experimental phase. These features provide a quantitative basis for comparing gastric activity patterns between different conditions and are further utilized for subsequent statistical analysis.

Table 4. Mean ± Standard Deviation of Extracted EGG Signal Features Across All Subjects

Condition	Channel	Phase	Dominant Frequency	Mean Frequency	Dominant Magnitude (Normalized)	Average Magnitude (Normalized)	Band Power (Normalized)
Pre-prandial	0	Pre	0.037 ±0.006	0.047 ±0.002	0.365 ±0.283	0.329 ±0.265	0.317 ±0.310
		Stim	0.037 ±0.007	0.047 ±0.002	0.485↑ ±0.215	0.495↑ ±0.352	0.550↑ ±0.306
		Post	0.035 ±0.006	0.047 ±0.002	0.221↓ ±0.215	0.204↓ ±0.186	0.132↓ ±0.121
	1	Pre	0.035 ±0.007	0.047 ±0.001	0.233 ±0.208	0.232 ±0.214	0.332 ±0.376
		Stim	0.035 ±0.007	0.047 ±0.001	0.483↑ ±0.322	0.471↑ ±0.332	0.502↑ ±0.374
		Post	0.039 ±0.006	0.048 ±0.002	0.240↓ ±0.214	0.241 ↓ ±0.210	0.165↓ ±0.173
Post-prandial	0	Pre	0.041 ±0.011	0.048 ±0.002	0.363 ±0.247	0.350 ±0.240	0.305 ±0.237
		Stim	0.043 ±0.009	0.048 ±0.002	0.397↑ ±0.240	0.384 ↑ ±0.231	0.358↑ ±0.190
		Post	0.038 ±0.008	0.048 ±0.002	0.313 ↓ ±0.220	0.301 ↓ ±0.210	0.337↓ ±0.185
	1	Pre	0.043 ±0.009	0.048 ±0.001	0.351 ±0.236	0.344 ±0.233	0.366 ±0.248
		Stim	0.039 ±0.008	0.048 ±0.002	0.382↑ ±0.229	0.372 ↑ ±0.223	0.381↑ ±0.243
		Post	0.039 ±0.008	0.048 ±0.001	0.296 ↓ ±0.215	0.288 ↓ ±0.206	0.253↓ ±0.228

↑ *Indicates an increasing trend from the Pre to Stim condition*
↓ *Indicates a decreasing trend from the Stim to Post condition.*

Table 4 summarizes the descriptive statistics (mean ± standard deviation) of the extracted EGG signal features for all subjects across the experimental phases (Pre, Stim, and Post) under both pre-prandial and post-prandial conditions. The dominant frequency values ranged from 0.032 ± 0.007 Hz to 0.044 ± 0.011 Hz across all phases, remaining within the typical gastric slow-wave range. The mean frequency showed little variation, with values consistently around 0.047 ± 0.002 Hz.

In contrast, magnitude-related features showed greater dispersion. The normalized dominant magnitude ranged from 0.221 ± 0.215 to 0.485 ± 0.335. The normalized average magnitude within the 0.03-0.07 Hz band ranged from 0.204 ± 0.186 to 0.495 ± 0.352, while the normalized band power ranged from 0.133 ± 0.121 to 0.550 ± 0.306. These magnitude-related features generally increased from the Pre phase to the Stim phase (↑) in both pre-prandial and post-prandial conditions, followed by a decrease in the Post phase (↓), indicating a temporary increase in gastric activity during stimulation. This indicates that VR exposure affects gastric electrical responses without altering their frequency.

Manuscript received 5 February 2026; Revised 15 March 2026; Accepted 20 April 2026; Available online 26 April 2026
Digital Object Identifier (**DOI**): https://doi.org/10.35882/jeeemi.v8i2.1531

Table 5. Correlation Between Motion Sickness and EGG Features

Condition	Channel	Phase	Dominant Frequency (r,p)	Mean Frequency (r,p)	Dominant Magnitude (Normalized)(r,p)	Average Magnitude (Normalized)(r,p)	Band Power (Normalized) (r,p)
Pre-prandial	0	Pre	0.586 (0.098)	-0.473 (0.199)	-0.539 (0.135)	-0.556 (0.120)	-0.574 (0.106)
		Stim	-0.421 (0.259)	-0.412 (0.271)	0.841 (0.005)*	0.742 (0.022)*	0.788 (0.012)*
		Post	-0.365 (0.334)	0.002 (0.996)	-0.269 (0.484)	-0.003 (0.995)	-0.085 (0.827)
	1	Pre	-0.382 (0.310)	-0.383 (0.309)	0.317 (0.406)	0.244 (0.527)	0.247 (0.523)
		Stim	-0.650 (0.058)	-0.561 (0.116)	0.429 (0.249)	0.383 (0.309)	0.444 (0.232)
		Post	-0.109 (0.780)	-0.019 (0.961)	-0.240 (0.534)	-0.127 (0.745)	-0.163 (0.676)
Post-prandial	0	Pre	0.375 (0.321)	-0.027 (0.945)	0.374 (0.321)	0.216 (0.576)	0.276 (0.472)
		Stim	0.354 (0.349)	0.224 (0.562)	-0.179 (0.646)	-0.430 (0.248)	-0.402 (0.283)
		Post	0.049 (0.900)	-0.129 (0.741)	-0.249 (0.518)	-0.298 (0.436)	-0.302 (0.429)
	1	Pre	0.302 (0.430)	-0.095 (0.807)	-0.197 (0.611)	-0.324 (0.396)	-0.187 (0.630)
		Stim	-0.360 (0.341)	0.079 (0.839)	0.151 (0.699)	0.204 (0.598)	0.109 (0.780)
		Post	-0.286 (0.456)	-0.120 (0.759)	-0.453 (0.221)	-0.474 (0.198)	-0.431 (0.247)

**p < 0.05 indicates statistical significance.*

D. Correlation Analysis Between Subjective Scores and EGG Features

This section presents the results of the correlation analysis between subjective evaluations, represented by Likert-scale scores (motion sickness and stressor), and physiological responses derived from EGG signal features across both pre-prandial and post-prandial phases. The analysis was conducted using Pearson's correlation coefficient to examine the strength and direction of the relationships, with statistical significance determined at a threshold of $p < 0.05$.

1. Motion sickness vs EGG

The correlation between motion sickness scores and EGG features is presented in Table 5 . Significant correlations were identified only during the pre-prandial Stim phase on channel 0. As shown in Table 5, statistically significant correlations were found only during the pre-prandial Stim phase on channel 0. These correlations were observed in three normalized magnitude features, namely dominant magnitude ($r = 0.841$; $p = 0.005$), average magnitude ($r = 0.742$; $p = 0.022$), and band power ($r = 0.788$; $p = 0.012$).

To illustrate these findings, Fig. 5 depicts the relationship between motion sickness scores and the three significant EGG features identified in Table 5. The scatter plots correspond to the pre-prandial Stim phase on channel 0, where Fig. 5(a) represents normalized dominant magnitude, Fig. 5(b) represents average magnitude, and Fig. 5 (c) represents band power. All three plots show a consistent upward trend, indicating a positive relationship between motion sickness scores and the extracted EGG features, where higher scores are associated with increased values of normalized dominant magnitude, average magnitude, and band power. This indicates that as the severity of motion

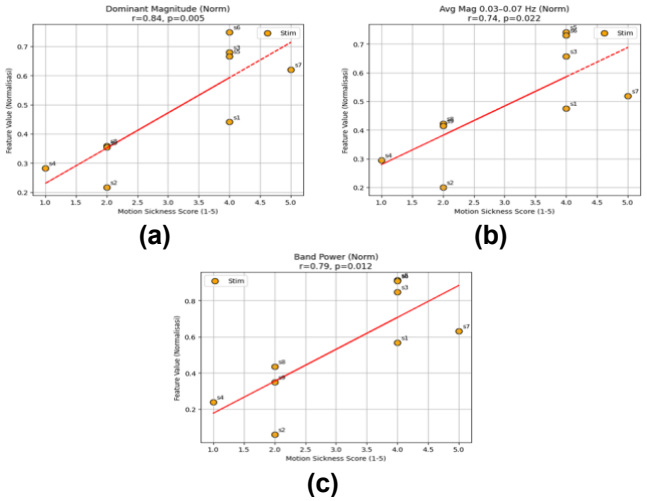

Fig. 5. Correlation Between Motion Sickness Scores and the Three Significant EGG Features During the Pre-prandial Stim Phase on Channel 0

sickness increases, the power of gastric slow-wave activity within the normogastric range also tends to

Manuscript received 5 February 2026; Revised 15 March 2026; Accepted 20 April 2026; Available online 26 April 2026
Digital Object Identifier (**DOI**): https://doi.org/10.35882/jeeemi.v8i2.1531

increase, consistent with the reported correlation coefficients (r = 0.841, r = 0.742, and r = 0.788). This finding supports the use of EGG features as indicators of motion sickness severity during VR exposure, showing their potential as reliable physiological markers.

2. Stressor vs EGG

The correlation between stressor Likert scores and EGG features is presented in Table 6. This analysis evaluates whether the recorded gastric activity within the 0.03-0.07 Hz range corresponds to the stressor levels reported by the subjects.

As shown in Table 6, most features, including dominant frequency and mean frequency, did not exhibit statistically significant correlations ($p > 0.05$). Significant correlations were observed only during the pre-prandial Stim phase on channel 0. In this phase, three normalized magnitude features showed strong positive correlations: dominant magnitude (r = 0.895, p = 0.001), average magnitude (r = 0.780, p = 0.013), and band power (r = 0.821, p = 0.007). These correlation coefficients are higher than those in the Pre and Post phases, while other features remain non-significant. Fig. 6 shows the relationship between stressor scores and the three significant EGG features.

The three significant features shown in Fig. 6 demonstrate positive correlations with stressor scores. The strongest correlation is observed for dominant magnitude (r = 0.895), followed by band power (r = 0.821) and average magnitude (r = 0.780). The scatter plots (a), (b), and (c) represent dominant magnitude, average magnitude, and band power, respectively, and show an increasing trend, where higher stressor scores are associated with greater values of the EGG magnitude features. Overall, magnitude-based EGG features exhibit stronger associations with subjective responses than frequency-based features.

Significant correlations were also identified between motion sickness scores and dominant magnitude (r = 0.841), average magnitude (r = 0.742), and band power (r = 0.788) during the pre-prandial Stim phase on channel 0. A similar pattern was observed for stressor

Table 6. Correlation Between Stressor and EGG Features

Condition	Channel	Phase	Dominant Frequency (r,p)	Mean Frequency (r,p)	Dominant Magnitude (Normalized)(r,p)	Average Magnitude (Normalized)(r,p)	Band Power (Normalized) (r,p)
Pre-prandial	0	Pre	0.274 (0.476)	-0.163 (0.675)	-0.578 (0.103)	-0.536 (0.137)	-0.531 (0.141)
		Stim	-0.388 (0.302)	-0.551 (0.124)	0.895 (0.001)*	0.780 (0.013)*	0.821 (0.007)*
		Post	-0.505 (0.166)	-0.119 (0.760)	-0.414 (0.268)	-0.308 (0.420)	-0.373 (0.322)
	1	Pre	-0.222 (0.565)	-0.142 (0.715)	-0.175 (0.653)	-0.192 (0.621)	-0.235 (0.544)
		Stim	-0.326 (0.392)	-0.342 (0.367)	0.328 (0.389)	0.278 (0.469)	0.351 (0.355)
		Post	-0.299 (0.435)	0.025 (0.948)	0.051 (0.896)	0.189 (0.627)	0.279 (0.467)
Post-prandial	0	Pre	0.236 (0.542)	-0.227 (0.557)	0.417 (0.265)	0.252 (0.513)	0.314 (0.410)
		Stim	0.250 (0.516)	0.065 (0.869)	-0.106 (0.786)	-0.408 (0.276)	-0.388 (0.302)
		Post	-0.206 (0.596)	0.099 (0.799)	-0.375 (0.320)	-0.057 (0.885)	-0.161 (0.679)
	1	Pre	0.299 (0.435)	-0.069 (0.861)	0.024 (0.951)	-0.042 (0.915)	0.108 (0.783)
		Stim	-0.513 (0.158)	0.069 (0.860)	0.140 (0.719)	0.153 (0.694)	0.038 (0.923)
		Post	-0.234 (0.545)	-0.214 (0.581)	-0.300 (0.433)	-0.307 (0.422)	-0.365 (0.334)

**p < 0.05 indicates statistical significance.*

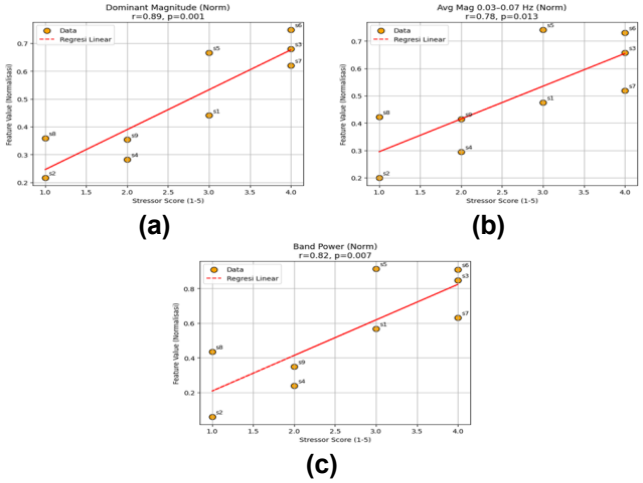

Fig. 6. Correlation Between Stressor Scores and the Three Significant EGG Features During the Pre-prandial Stim Phase on Channel 0

Manuscript received 5 February 2026; Revised 15 March 2026; Accepted 20 April 2026; Available online 26 April 2026
Digital Object Identifier (**DOI**): https://doi.org/10.35882/jeeemi.v8i2.1531

scores, with dominant magnitude (r = 0.895), band power (r = 0.821), and average magnitude (r = 0.780). In contrast, dominant frequency and mean frequency remained relatively stable across phases and did not show statistically significant correlations (p > 0.05), indicating that magnitude-based features are more sensitive to variations in subjective responses under the experimental conditions.

IV. Discussion

This study aims to investigate gastric myoelectrical responses associated with motion sickness and perceived stress induced by immersive Virtual Reality (VR) exposure using electrogastrogram (EGG) signal analysis.

A. Main Physiological Findings of EGG Responses

The results indicate that magnitude-based EGG features-including dominant magnitude, average magnitude, and band power-are more sensitive in capturing physiological responses compared to frequency-based features. Significant positive correlations were observed between EGG magnitude features and motion sickness, including dominant magnitude (r = 0.841, p = 0.005), average magnitude (r = 0.742, p = 0.022), and band power (r = 0.788, p = 0.012). Similarly, strong correlations were found between EGG features and stressor levels, with dominant magnitude (r = 0.895, p = 0.001), average magnitude (r = 0.780, p = 0.013), and band power (r = 0.821, p = 0.007). In addition, motion sickness and stressor scores were strongly correlated (r = 0.86, p = 0.003). In contrast, frequency-based features remained stable within the normogastric range (0.03-0.07 Hz), with dominant frequency varying between 0.032 ± 0.007 Hz and 0.044 ± 0.011 Hz, and mean frequency around 0.047 ± 0.002 Hz. These values are consistent with the normal gastric slow-wave frequency of approximately 2-4 cycles per minute (cpm) reported in previous studies [25], [38].

Although frequency characteristics remained stable, magnitude-based features showed clear changes across phases. In the pre-prandial condition (channel 0), dominant magnitude increased from 0.365 ± 0.283 (Pre) to 0.485 ± 0.215 (Stim) and then decreased to 0.221 ± 0.215 (Post) (Δ = 0.120). Similar patterns were observed for average magnitude (0.329 → 0.495 → 0.204) and band power (0.317 → 0.550 → 0.132). This increase-decrease pattern reflects a transient enhancement of gastric electrical intensity during VR stimulation followed by recovery, consistent with motion sickness studies reporting peak physiological activation during sensory exposure [12], [22]. The VR stimulus used in this study, the Epic Roller Coaster simulation, is known to induce strong visual-vestibular conflict due to rapid motion and frequent changes in perspective [30-31]. These characteristics likely contributed to the observed increases in magnitude-based EGG features, with band power reaching values up to 0.550 ± 0.306 during the stimulation phase. However, these responses may be specific to high-motion VR environments, and less dynamic applications, such as virtual learning or training, may produce weaker physiological effects.

B. Relationship Between Motion Sickness and Stressor Responses

The analysis indicates a consistent and statistically significant association between motion sickness severity and perceived stressor intensity across experimental conditions. In the pre-prandial condition, the strongest correlation was observed during the stimulation phase (r = 0.85, p = 0.004), followed by the post-stimulation phase (r = 0.68, p = 0.044). Similarly, in the post-prandial condition, strong correlations were identified during the stimulation phase (r = 0.86, p = 0.003) and the pre-phase (r = 0.81, p = 0.008).

These findings demonstrate that higher levels of motion sickness are consistently associated with increased perceived stress, particularly during VR exposure. This supports previous studies indicating that motion sickness is closely related to acute stress responses, including elevated physiological arousal and subjective tension [47], and that psychological factors such as stress and anxiety may exacerbate motion sickness severity [48]. From a mechanistic perspective, this relationship may reflect the interaction between sensory conflict and autonomic regulation, where visual-vestibular mismatch not only induces nausea but also amplifies stress-related responses. In contrast, no significant relationship was found between Body Mass Index (BMI) and motion sickness scores across all experimental phases. This suggests that susceptibility to motion sickness is more strongly influenced by sensory integration mechanisms rather than anthropometric factors, as motion sickness primarily arises from conflicts between visual and vestibular inputs.

C. Physiological Interpretation and Implications

Further analysis shows that significant correlations between EGG features and motion sickness were observed specifically in the pre-prandial stimulation phase at channel 0, where dominant magnitude, average magnitude, and band power demonstrated strong positive associations with subjective motion sickness scores. These findings are consistent with the observed increase in magnitude values during the stimulation phase, indicating that gastric electrical activity becomes more responsive under VR-induced sensory conflict. A comparison between physiological states reveals that gastric responses are more

Manuscript received 5 February 2026; Revised 15 March 2026; Accepted 20 April 2026; Available online 26 April 2026
Digital Object Identifier (**DOI**): https://doi.org/10.35882/jeeemi.v8i2.1531

pronounced under pre-prandial conditions. The increase in dominant magnitude during stimulation was higher in the pre-prandial state (Δ = 0.120) compared to the post-prandial condition (Δ = 0.034). This suggests that gastric electrical activity is more sensitive during fasting, likely due to autonomic modulation associated with the migrating motor complex (MMC). In contrast, post-prandial activity is dominated by digestive processes, which may reduce responsiveness to external stimuli [38], [46], [47].

Differences in electrode placement may also explain why channel 1 did not exhibit significant correlations, as spatial variations in gastric electrical activity can influence signal sensitivity and amplitude detection [38]. From a broader physiological perspective, these findings can be interpreted within the framework of the gut-brain axis, where sensory conflict during VR exposure influences autonomic pathways regulating gastrointestinal activity. Neural interactions between the brainstem and the gastrointestinal system, mediated through pathways such as the vagus nerve, may explain the increase in magnitude-based EGG features observed during stimulation [48], [49]. Overall, this study highlights the potential of magnitude-based EGG features as objective physiological indicators for monitoring motion sickness and stress responses in immersive VR environments. However, several limitations should be considered, including the relatively small sample size and the susceptibility of EGG signals to artifacts such as respiration, body movement, and electrode variability. Future studies should involve larger and more diverse participant populations and integrate multimodal physiological signals, such as EEG, electrodermal activity (EDA), and heart rate variability (HRV), to provide a more comprehensive understanding of gut-brain interactions and support the development of adaptive VR systems.

V. Conclusion

This study investigates gastric myoelectrical responses associated with motion sickness and perceived stress induced by immersive Virtual Reality (VR) using electrogastrogram (EGG) signals. The results confirm that VR induces moderate to high discomfort (Likert scores 3-5), which can be evaluated using combined objective (EGG with FFT) and subjective approaches. Among five frequency-domain features (0.03-0.07 Hz), dominant magnitude, average magnitude, and band power were identified as the most sensitive indicators, particularly at channel 0 during pre-prandial stimulation, showing significant correlations with motion sickness ($r = 0.841$, $p = 0.005$; $r = 0.742$, $p = 0.022$; $r = 0.788$, $p = 0.012$) and stress ($r = 0.895$, $p = 0.001$; $r = 0.780$, $p = 0.013$; $r = 0.821$, $p = 0.007$). Subjective findings indicate higher sensitivity in pre-prandial conditions (55.6%) compared to post-prandial (44.4%), supported by greater dominant magnitude changes (Δ = 0.120 vs 0.034). Furthermore, the lower corpus-antrum-pylorus region (channel 0) provides the most representative signals, highlighting the importance of electrode placement. However, this study is limited by a relatively small sample size; future work should include larger populations and integrate multimodal signals (EEG, EDA, HRV) to enhance analysis and support adaptive VR systems.

Acknowledgment

The authors would like to express their gratitude to the Faculty of Industrial Technology and the Department of Electrical Engineering, Universitas Islam Indonesia, for their support in this research.

References

[1] O. Escallada, G. Lasa, M. Mazmela, A. Apraiz, N. Osa, and H. Nguyen Ngoc, “Assessing Human Factors in Virtual Reality Environments for Industry 5.0: A Comprehensive Review of Factors, Metrics, Techniques, and Future Opportunities,” *Information*, vol. 16, no. 1, p. 35, Jan. 2025, doi: 10.3390/info16010035.

[2] C. E. Mendoza-Ramírez, J. C. Tudon-Martinez, L. C. Félix-Herrán, J. D. J. Lozoya-Santos, and A. Vargas-Martínez, “Augmented Reality: Survey,” *Applied Sciences*, vol. 13, no. 18, p. 10491, Jan. 2023, doi: 10.3390/app131810491.

[3] X. Fan, J. Xun, L. Dolega, and L. Xiong, “The Role of Augmented and Virtual Reality in Shaping Retail Marketing: A Meta-Analysis,” *Sustainability*, vol. 17, no. 2, p. 728, Jan. 2025, doi: 10.3390/su17020728.

[4] R. Cioffi and A. V. Lubetzky, “BOXVR Versus Guided YouTube Boxing for Stress, Anxiety, and Cognitive Performance in Adolescents: A Pilot Randomized Controlled Trial,” *Games Health J*, vol. 12, no. 3, pp. 259-268, Jun. 2023, doi: 10.1089/g4h.2022.0202.

[5] D. M. Yoon, S. H. Han, I. Park, and T. S. Chung, “Analyzing VR Game User Experience by Genre: A Text-Mining Approach on Meta Quest Store Reviews,” *Electronics*, vol. 13, no. 19, Oct. 2024, doi: 10.3390/electronics13193913.

[6] X. Song, N. M. Ali, M.H. M. Salim, and M. Y. Rezaldi, “A Literature Review of Virtual Reality Exergames for Older Adults: Enhancing Physical, Cognitive, and Social Health,” *Applied Sciences*, vol. 15, no. 1, Jan. 2025, doi: 10.3390/app15010351.

[7] M. Soliman, A. Pesyridis, D. Dalaymani-Zad, M.

Manuscript received 5 February 2026; Revised 15 March 2026; Accepted 20 April 2026; Available online 26 April 2026
Digital Object Identifier (**DOI**): https://doi.org/10.35882/jeeemi.v8i2.1531

Gronfula, and M. Kourmpetis, "The Application of Virtual Reality in Engineering Education," *Applied Sciences*, vol. 11, no. 6, p. 2879, Jan. 2021, doi: 10.3390/app11062879.

[8] A. M. Al-Ansi, M. Jaboob, A. Garad, and A. Al-Ansi, "Analyzing augmented reality (AR) and virtual reality (VR) recent development in education," *Social Sciences & Humanities Open*, vol. 8, no. 1, p. 100532, Jan. 2023, doi: 10.1016/j.ssaho.2023.100532.

[9] R. R. McKnight, C. A. Pean, J. S. Buck, J. S. Hwang, J. R. Hsu, and S. N. Pierrie, "Virtual Reality and Augmented Reality-Translating Surgical Training into Surgical Technique," *Curr Rev Musculoskelet Med*, vol. 13, no. 6, pp. 663-674, Dec. 2020, doi: 10.1007/s12178-020-09667-3.

[10] T. Finseth, M. C. Dorneich, N. Keren, W. D. Franke, and S. B. Vardeman, "Manipulating Stress Responses during Spaceflight Training with Virtual Stressors," *Applied Sciences*, vol. 12, no. 5, p. 2289, Jan. 2022, doi: 10.3390/app12052289.

[11] G. Lucas, A. Kemeny, D. Paillot, and F. Colombet, "A simulation sickness study on a driving simulator equipped with a vibration platform," *Transportation Research Part F: Traffic Psychology and Behaviour*, vol. 68, pp. 15-22, Jan. 2020, doi: 10.1016/j.trf.2019.11.011.

[12] N. B. Popović, N. Miljković, K. Stojmenova, G. Jakus, M. Prodanov, and J. Sodnik, "Lessons Learned: Gastric Motility Assessment During Driving Simulation," *Sensors*, vol. 19, no. 14, p. 3175, Jan. 2019, doi: 10.3390/s19143175.

[13] A. Javaid, S. Rasool, and A. Maqsood, "Analysis of Visual and Vestibular Information on Motion Sickness in Flight Simulation," *Aerospace*, vol. 11, no. 2, Feb. 2024, doi: 10.3390/aerospace11020139.

[14] A. Koohestani, D. Nahavandi, H. Asadi, P. M. Kebria, A. Khosravi, R. Alizadehsani, et al., "A Knowledge Discovery in Motion Sickness: A Comprehensive Literature Review," *IEEE Access*, vol. 7, pp. 1-16, 2019, doi: 10.1109/ACCESS.2019.2922993.

[15] F. Ghasemi, D. Q. Beversdorf, and K. C. Herman, "Stress and stress responses: A narrative literature review from physiological mechanisms to intervention approaches," *Journal of Pacific Rim Psychology*, vol. 18, pp. 1-20, May 2024, doi: 10.1177/18344909241289222.

[16] H. Kim, D. J. Kim, W. H. Chung, K. A. Park, J. D. K. Kim, D. Kim, K. Kim, and H. J. Jeon, "Clinical predictors of cybersickness in virtual reality (VR) among highly stressed people," *Scientific Reports*, vol. 11, no. 1, p. 12139, Jun. 2021, doi: 10.1038/s41598-021-91573-w.

[17] H. Oh and W. Son, "Cybersickness and Its Severity Arising from Virtual Reality Content: A Comprehensive Study," *Sensors*, vol. 22, no. 4, p. 1314, Feb. 2022, doi: 10.3390/s22041314.

[18] M. Jamil, H. Hadiyanto, and R. Sanjaya, "Identification and Evaluation of Cybersickness Impact of Mixed Reality Simulator (MRSi) System," *Journal Européen des Systèmes Automatisés*, vol. 58, no. 1, pp. 105-113, Jan. 2025, doi: 10.18280/jesa.580112.

[19] L. Bareišytė, S. Slatman, J. Austin, M. Rosema, I. V. Sintemaartensdijk, S. Watson, et al., "Questionnaires for evaluating virtual reality: A systematic scoping review," *Computers in Human Behavior Reports*, vol. 16, p. 100505, Dec. 2024, doi: 10.1016/j.chbr.2024.100505.

[20] A. T. Alabi and M. O. Jelili, "Clarifying likert scale misconceptions for improved application in urban studies," *Qual Quant*, vol. 57, no. 2, pp. 1337-1350, Apr. 2023, doi: 10.1007/s11135-022-01415-8.

[21] A. J. Martingano, E. Brown, S. H. Telaak, A. P. Dolwick, and S. Persky, "Cybersickness Variability by Race: Findings From 6 Studies and a Mini Meta-analysis," *J Med Internet Res*, vol. 24, no. 6, pp. 1-14, Jun. 2022, doi: 10.2196/36843.

[22] T. Gruden, N. B. Popović, K. Stojmenova, G. Jakus, N. Miljković, S. Tomažič, et al., "Electrogastrography in Autonomous Vehicles-An Objective Method for Assessment of Motion Sickness in Simulated Driving Environments," *Sensors*, vol. 21, no. 2, p. 550, Jan. 2021, doi: 10.3390/s21020550.

[23] J. Wang, H.-N. Liang, D. Monteiro, W. Xu, and J. Xiao, "Real-Time Prediction of Simulator Sickness in Virtual Reality Games," *IEEE Transactions on Games*, vol. 15, no. 2, pp. 252-261, Jun. 2023, doi: 10.1109/TG.2022.3178539.

[24] J. Smyth, S. Birrell, R. Woodman, and P. Jennings, "Exploring the utility of EDA and skin temperature as individual physiological correlates of motion sickness," *Applied Ergonomics*, vol. 92, p. 103315, Apr. 2021, doi: 10.1016/j.apergo.2020.103315.

[25] A. Sahroni, I. Miladiyah, S. Adinandra, P. R. Sofyan, L. Anora, and Mhd. Hanafi, "Single Channel Electrogastrogram Frequency Domain Analysis and Correspondence to Brain Activity in a Resting State Condition," *Journal of*

Manuscript received 5 February 2026; Revised 15 March 2026; Accepted 20 April 2026; Available online 26 April 2026
Digital Object Identifier (**DOI**): https://doi.org/10.35882/jeeemi.v8i2.1531

Electronics, Electromedical Engineering, and Medical Informatics, vol. 7, no. 1, pp. 243-252, Nov. 2024, doi: 10.35882/jeeemi.v7i1.590.

[26] R. Liu, M. Xu, Y. Zhang, E. Peli, and A. D. Hwang, "A Pilot Study on EEG-Based Evaluation of Visually Induced Motion Sickness," *J. Imaging Sci. Technol.*, vol. 64, no. 2, pp. 20501-1-20501-10, Mar. 2020, doi: 10.2352/J.ImagingSci.Technol.2020.64.2.020501.

[27] Y. S. Kim, J. Won, S.-W. Jang, and J. Ko, "Effects of Cybersickness Caused by Head-Mounted Display-Based Virtual Reality on Physiological Responses: Cross-sectional Study," *JMIR Serious Games*, vol. 10, no. 4, p. e37938, Oct. 2022, doi: 10.2196/37938.

[28] A. K Kasap and B. Kurt, "Exploring the Correlation of Physiological Stress Signals with Student Exam Performance: A Preliminary Study," *Appl. Psychophysiol. Biofeedback*, vol. 50, no. 1, pp. 149-164, Mar. 2025, doi: 10.1007/s10484-025-09685-2.

[29] J. Jih, A. Mukherjea, E. Vittinghoff, T. T. Nguyen, J. Y. Tsoh, Y. Fukuoka, et al., "Using appropriate body mass index cut points for overweight and obesity among Asian Americans," *Preventive Medicine*, vol. 65, pp. 1-6, Aug. 2014, doi: 10.1016/j.ypmed.2014.04.010.

[30] C. F. Hasibuan, B. Hartono, and T. Wijayanto, "Effect of prior gaming experience on cybersickness symptoms in a virtual reality environment," *Virtual Reality & Intelligent Hardware*, vol. 7, no. 5, pp. 468-482, Oct. 2025, doi: 10.1016/j.vrih.2025.06.003.

[31] S. Thorp, A. Sævild Ree, and S. Grassini, "Temporal Development of Sense of Presence and Cybersickness during an Immersive VR Experience," *Multimodal Technologies and Interaction*, vol. 6, no. 5, p. 31, May 2022, doi: 10.3390/mti6050031.

[32] U. Laessoe, S. Abrahamsen, S. Zepernick, A. Raunsbaek, and C. Stensen, "Motion sickness and cybersickness - Sensory mismatch," *Physiology & Behavior*, vol. 258, p. 114015, Jan. 2023, doi: 10.1016/j.physbeh.2022.114015.

[33] S. Qi and M. Menozzi, "Effects of cybersickness mitigation methods on behavior: a comparative study based on the skill-rule-knowledge model," *Virtual Reality*, vol. 28, no. 4, p. 171, Nov. 2024, doi: 10.1007/s10055-024-01071-3.

[34] E. Jochmann, T. Jochmann, M. Weber, K. Weigel, and C. Klingner, "Impact of sensorimotor mismatch on virtual reality sickness and user experience: age-related differences in a randomized trial," *J Neuroeng Rehabil*, vol. 22, p. 143, Jul. 2025, doi: 10.1186/s12984-025-01677-x.

[35] G. Aikawa, T. Hoshino, H. Sakuramoto, A. Ouchi, M.Ikeda, et al., "Quantitative visualization of gastrointestinal motility in critically ill patients using a non-invasive single-channel electro amplifier: A prospective observational cohort feasibility study," *Journal of Critical Care*, vol. 87, p. 155031, Jun. 2025, doi: 10.1016/j.jcrc.2025.155031.

[36] A. A. Kafee and Y. Kayar, "Electrogastrography in patients with gastric motility disorders," *Proc Inst Mech Eng H*, vol. 238, no. 1, pp. 22-32, Jan. 2024, doi: 10.1177/09544119231212269.

[37] N. Wolpert, I. Rebollo, and C. Tallon-Baudry, "Electrogastrography for psychophysiological research: Practical considerations, analysis pipeline, and normative data in a large sample," *Psychophysiology*, vol. 57, no. 9, pp. 1-25, Sep. 2020, doi: 10.1111/psyp.13599.

[38] D. Oczka, M. Augustynek, M. Penhaker, and J. Kubicek, "Electrogastrography measurement systems and analysis methods used in clinical practice and research: comprehensive review," *Front Med (Lausanne)*, vol. 11, pp. 1-18, Jul. 2024, doi: 10.3389/fmed.2024.1369753.

[39] R. Liu, "Utilizing Fast Fourier Transform in the processing of biomedical signals: An analytical approach," *Theoretical and Natural Science*, vol. 38, pp. 154-159, 2024, doi: 10.54254/2753-8818/38/20240589.

[40] J. C. Erickson, C. Obioha, A. Goodale, L. A. Bradshaw, and W. O. Richards, "Detection of Small Bowel Slow-Wave Frequencies From Noninvasive Biomagnetic Measurements," *IEEE Transactions on Biomedical Engineering*, vol. 56, no. 9, pp. 2181-2189, Sep. 2009, doi: 10.1109/TBME.2009.2024087.

[41] S.-Y. Park and D.-K. Koo, "The Impact of Virtual Reality Content Characteristics on Cybersickness and Head Movement Patterns," *Sensors*, vol. 25, no. 1, p. 215, Jan. 2025, doi: 10.3390/s25010215.

[42] L. Eudave and M. Martínez, "To VR or not to VR: assessing cybersickness in navigational tasks at different levels of immersion," *Front. Virtual Real.*, vol. 6, pp. 1-13, Feb. 2025, doi: 10.3389/frvir.2025.1518735.

[43] M. M. Mottalib, J. C. Jones-Smith, B. Sheridan, and R. Beheshti, "Subtyping Patients With Chronic Disease Using Longitudinal BMI Patterns," *IEEE J Biomed Health Inform*, vol. 27, no. 4, pp. 2083-2093, Apr. 2023, doi:

Manuscript received 5 February 2026; Revised 15 March 2026; Accepted 20 April 2026; Available online 26 April 2026
Digital Object Identifier (**DOI**): https://doi.org/10.35882/jeeemi.v8i2.1531

10.1109/JBHI.2023.3237753.

[44] P. P. Balasubramani, A. Walke, G. Grennan, A. Parley, S. Purpura, D. Ramanathan, et al., "Simultaneous Gut-Brain Electrophysiology Shows Cognition and Satiety Specific Coupling," *Sensors*, vol. 22, no. 23, p. 9242, Nov. 2022, doi: 10.3390/s22239242.

[45] A. A. Gharibans, S. Kim, D. Kunkel, and T. P. Coleman, "High-Resolution Electrogastrogram: A Novel, Noninvasive Method for Determining Gastric Slow-Wave Direction and Speed," *IEEE Trans Biomed Eng*, vol. 64, no. 4, pp. 807-815, Apr. 2017, doi: 10.1109/TBME.2016.2579310.

[46] C. Jacob, E. Olliges, A. Haile, V. Hoffmann, B. Jacobi, L. Steinkopf, et al., "Placebo effects on nausea and motion sickness are resistant to experimentally-induced stress," *Scientific Reports*, vol. 13, no. 1, pp. 1-11, Jun. 2023, doi: 10.1038/s41598-023-36296-w.

[47] D. Stelling, M. Hermes, G. Huelmann, J. Mittelstadt, D. Niedermeier, K. Schudlik, et al., "Individual differences in the temporal progression of motion sickness and anxiety: the role of passengers' trait anxiety and motion sickness history," *Ergonomics*, vol. 64, no. 8, pp. 1062-1071, Aug. 2021, doi: 10.1080/00140139.2021.1886334.

[48] A. Furgała, K. Ciesielczyk, M. Przybylska-Feluś, K. Jabłoński, K. Gil, and M. Zwolińska-Wcisło, "Postprandial effect of gastrointestinal hormones and gastric activity in patients with irritable bowel syndrome," *Scientific Reports*, vol. 13, no. 1, p. 9420, Jun. 2023, doi: 10.1038/s41598-023-36445-1.

[49] M. Przybylska-Feluś, A. Furgała, K. Ciesielczyk, K. Gil, and M. Zwolińska-Wcisło, "Disturbances of autonomic nervous system and gastric activity in response to visceral stimulation in functional dyspepsia patients," *Prz Gastroenterol*, vol. 20, no. 3, pp. 284-293, 2025, doi: 10.5114/pg.2025.154638.

Author Biography

Mhd. Hanafi graduated from the Department of Electrical Engineering at Universitas Islam Indonesia. He obtained his bachelor's degree in Informatics Engineering (S.Kom) from Abdurrab University, Pekanbaru, and his master's degree (M.T.) in Electrical Engineering from Universitas Islam Indonesia. His research experience includes indoor positioning system instrumentation, smart systems, Internet of Things (IoT), medical image processing, and human physiological signal processing, such as EEG, EGG, ECG, EOG, and EMG. He also has a strong interest in artificial intelligence (AI) and its applications in biomedical engineering. He has been actively involved in several research projects and continues to explore the integration of AI techniques into biomedical and engineering systems to improve performance, reliability, and accuracy.

Alvin Sahroni received his B.Eng. degree in Electrical Engineering from Universitas Islam Indonesia, Yogyakarta, in 2008, followed by his M.Eng. degree from Universitas Gadjah Mada, Indonesia. During his master's studies, he participated in a joint program involving Gadjah Mada University, Bandung Institute of Technology, and Karlsruhe Institute of Technology, Germany, in 2011. He obtained his doctoral degree from Kumamoto University, Japan, in 2017. His research focuses on physiological signal analysis for applications in psychology, medicine, and rehabilitation. He has also been a technology enthusiast and machine learning researcher since 2014. Currently, he is involved in biosignal processing research for stress detection and related applications.

Sri Kusumadewi is a lecturer in the Department of Informatics, Faculty of Industrial Technology, at the Universitas Islam Indonesia. She earned her Bachelor's degree (S.Si.) in Computer Science, Master's degree (M.T.) in Information Technology, and Doctoral degree (Dr.) in Computer Science, all from Gadjah Mada University. Her research interests primarily include medical informatics and decision support systems. In addition to teaching and conducting research, she has authored several textbooks in the field of artificial intelligence. She has also contributed to numerous academic publications and actively participates in collaborative research projects in the areas of intelligent systems and healthcare technology.

Hendra Setiawan is a lecturer in the Department of Electrical Engineering, Faculty of Industrial Technology, at the Universitas Islam Indonesia. He received his Bachelor of Engineering (S.T.) degree from Universitas Gadjah Mada, Indonesia, followed by his Master of Engineering (M.T.)

Manuscript received 5 February 2026; Revised 15 March 2026; Accepted 20 April 2026; Available online 26 April 2026
Digital Object Identifier (**DOI**): https://doi.org/10.35882/jeeemi.v8i2.1531

degree from the Bandung Institute of Technology, Indonesia. He later completed his Doctor of Engineering (Dr. Eng.) at the Kyushu Institute of Technology, Japan. His areas of expertise include electronics, FPGA technology, signal processing, and wireless communication at the physical layer. His current research activities focus on the development of embedded systems, hardware implementation, and wireless communication technologies.

Firdaus is a lecturer in the Department of Electrical Engineering, Faculty of Industrial Technology, at the Universitas Islam Indonesia. He completed his Bachelor of Engineering (S.T.) degree at Universitas Gadjah Mada, Indonesia, followed by his Master of Engineering (M.T.) degree from Institut Teknologi Telkom, Indonesia. He later earned his Ph.D. from Universiti Teknologi Malaysia, Malaysia. His areas of expertise include wireless communication, wireless sensor networks, indoor positioning, and telemonitoring. His current research focuses on the development of wireless-based systems and intelligent sensing technologies for real-time monitoring, automation applications, and smart environment integration.

Manuscript received 5 February 2026; Revised 15 March 2026; Accepted 20 April 2026; Available online 26 April 2026
Digital Object Identifier (**DOI**): https://doi.org/10.35882/jeeemi.v8i2.1531